OPEN ACCESS
Freely Available Online

JOURNAL OF ADVANCES IN NANOTECHNOLOGY
ISSN NO: 2689-2855

Research

DOI: 10.14302/issn.2689-2855.jan-21-3745

Assessment of Physical, Thermal and Spectral Properties of Consciousness Energy Treated Cholecalciferol

Mahendra Kumar Trivedi[1], Snehasis Jana[2, *]

[1]Trivedi Global, Inc., Henderson, Nevada, USA

[2]Trivedi Science Research Laboratory Pvt. Ltd., Thane (W), India

Abstract

Cholecalciferol (vitamin D_3) is used nowadays in nutraceuticals regarding the prevention and treatment of vitamin D deficiency and associated diseases. This study was done to analyse the effect of the Trivedi Effect® - Energy of Consciousness Treatment on the physicochemical, thermal, and spectral properties of cholecalciferol using PSA, PXRD, DSC, TGA/DTG, FT-IR, and UV-Vis analysis. For this study, the cholecalciferol sample was divided into control/ untreated and Biofield Energy Treated vitamin D_3. The treated vitamin D_3 sample received Biofield Energy Treatment (the Trivedi Effect®) remotely for ~3 minutes by Mr. Mahendra Kumar Trivedi, who was located in the USA, while the test samples were located in the research laboratory in India. The treated sample was designated as the Biofield Energy Treated sample. The PSA analysis showed that the particle size values at d_{10}, d_{50}, d_{90}, and D(4, 3) of the treated sample were significantly decreased by 5.80%, 16.49%, 17.52%, and 16.23%, respectively compared to the control sample. However, the specific surface area of the treated cholecalciferol was significantly increased by 7.26% compared to the control sample. Besides, the PXRD analysis revealed that the relative intensities regarding the characteristic diffraction peaks in the treated sample were significantly altered from -42.56% to 22.42%, along with -41.69% to 72.71% alterations in the crystallite sizes, compared with the control sample. Also, the treated sample showed 2.80% decrease in the average crystallite size. The DSC analysis showed a slight increase (0.24%) in the melting point of the treated sample along with 3.68% increase in the latent heat of fusion (ΔH) compared to the control sample. Also, the decomposition temperature of the treated sample was decreased by 0.29%, whereas the ΔH was increased by 5.79%, compared to the control sample. Moreover, the TGA/DTG analysis revealed the significant decrease in weight loss in the 1st and 3rd step of degradation of the treated sample by 18.58% and 89.81%, respectively, along with 1.83% increase in the maximum thermal degradation temperature compared with the control sample. Overall, the thermal stability of the treated cholecalciferol sample was observed to be increased in comparison to the control sample. Thus, the Trivedi Effect® might be used to produce a different polymorph of cholecalciferol, which possesses the improved qualities in terms of appearance, dissolution, absorption, bioavailability, and thermal stability as compared with the untreated sample. Thus, the Biofield Energy Treated cholecalciferol might be used in designing of better nutraceutical and pharmaceutical formulations possessing improved therapeutic response regarding the treatment of vitamin D deficiency associated diseases.

OPEN ACCESS
Freely Available Online

OpenAccessPub

Corresponding author: Snehasis Jana, Trivedi Science Research Laboratory Pvt. Ltd., Thane (W), India. Tel: +91-022-25811234

Keywords: Cholecalciferol, The Trivedi Effect®, Energy of Consciousness Treatment, PSA, PXRD, DSC, TGA

Received: Jan 23, 2021 **Accepted:** Feb 15, 2021 **Published:** Feb 15, 2021

Editor: Adeshina Adekeye, Nigeria.

Introduction

Vitamin D is an important nutrient for optimum bone health and calcium homeostasis that can control the skeletal disease of bone thinning and compromised bone strength, osteoporosis, *etc*. [1, 2]. Vitamin D and calcium have been well recognized and important nutrients required for bone health and maintenance. Data suggests that for optimal care in case of bone loss, vitamin D and calcium are the preferred choices. However, more than 50% women were reported with an inadequate level of vitamin D, and approximately 90% women are not getting enough calcium in their diet or supplementation [3]. The vitamin D main circulating form is 25-hydroxyvitamin D (25[OH]D) (calcidiol) that requires activation by renal 1-α-hydroxylase in order to form the metabolically active form of vitamin D, 1, 25-dihydroxvitamin D (1,25$[OH]_2$D) (calcitriol) [4].

However, the skin has the capacity to produce vitamin D through robust photolytic process acting on a derivative of cholesterol (7-dehydrocholesterol) in order to form previtamin D, which is slowly isomerized into vitamin D_3 [5]. An important fact about vitamin D is its requirement throughout life. Besides, it's an important role in the formation of bone; vitamin D is likely to play an important role in several other physiologic systems. However, vitamin D plays important multiple roles in many degenerative diseases, functions of muscles, brain, lungs, liver, kidneys, heart, immune system, pancreas, large and small intestines and also work as an anticancer agent [6]. Vitamin D receptor (VDR) has been reported to be present in nearly every tissue along with several thousands of VDR binding sites throughout the genome, which accelerates the interest in vitamin D and its impact on multiple biologic processes. Insufficient level (25OHD below 5 ng/ mLor 12 nM) of vitamin D leads to rickets in children and osteomalacia in adults. However, the recent report suggesting that in order to prevent bone disease and fractures in growing consensus, 20 ng/mL (50 nM) was sufficient for 97.5% of the population. In addition, 600 IU of vitamin D was thought to be sufficient in age between 1 to 70 years, although 4,000 IU of vitamin D was considered safe [7, 8]. Vitamin D deficiency results in memory loss, bone pain, arthritis, multiple sclerosis, bone fracture, cancer, diabetes mellitus, mental disorders, soft bones that may result in deformities, cardiovascular diseases, unexplained fatigue, inflammations, infections, stress, aging, muscle weakness, Parkinson's and Alzheimer's diseases. In order to prevent the insufficient level, nutraceuticals, calcium supplements are required with high stability. Thus, vitamin D_3 stability, sensitivity, mechanism of action, its absorption in the body plays an important role that directly affected its sufficient level [9, 10].

The stability of Vitamin D_3 could be a reason for concern regarding its absorption and bioavailability as it is air and light sensitive compound [11, 12]. However, the physicochemical properties such as particle size, melting and decomposition behaviour may affect the stability profile [13]. Hence several researches have been emphasized mainly to improve such parameters and thereby the stability of the compound. Nowadays, the Biofield Energy Treatment (the Trivedi Effect®) has also been known for its profound impact on the physicochemical properties of the drug and its thermal behaviour [14-16]. Every living organism possesses an infinite and para-dimensional unique energy, which

surrounds the body in the form of the electromagnetic field and known as the Biofield Energy. There are several Energy Therapies in the world that are based on the Biofield Energy (Putative Energy Fields), and they have a significant effect on various disease conditions [17]. Therefore, such Energy therapies are recommended by the National Institute of Health/ National Center for Complementary and Alternative Medicine (NIH/NCCAM) under the category of Complementary and Alternative Medicine (CAM) [18]. The Trivedi Effect®-Consciousness Energy has also been known in this field due to its impact on the properties of metals and ceramics [19-21], pharmaceutical products [22, 23], nutraceuticals [24, 25], and organic compounds [26, 27]. Impact of the Biofield Energy Treatment has also been reported in the field of skin health [28, 29], agricultural science [30, 31], and livestock [32]. Thus, this study was aimed to determine the impact of the Biofield Energy Treatment on the physicochemical, thermal and spectral properties of cholecalciferol with the help of various analytical techniques such as PSA, PXRD, DSC, TGA/DTG, FT-IR spectrometry, and UV-vis spectroscopy.

Materials and Methods

Chemicals and Reagents

Cholecalciferol was purchased from Sigma-Aldrich, India. All other chemicals used during the experiments were of analytical grade available in India.

Consciousness Energy Healing Treatment Strategies

The vitamin D_3 sample was divided into two parts. One part of the vitamin D_3 was considered as a control/untreated sample, which was not received the Biofield Energy Treatment. The second part of the vitamin D_3 sample was received the Trivedi Effect®-Consciousness Energy Treatment remotely under standard laboratory conditions for ~3 minutes by Mr. Mahendra Kumar Trivedi and termed as the Biofield Energy Treated vitamin D_3. Mr. Trivedi was located in the USA, while the test samples were located in the research laboratory in India. This Biofield Energy Treatment was provided through the Mahendra Trivedi's unique energy transmission process to the test item. Consequently, the Control sample was subjected to a "sham" healer (who did not have any knowledge about the Biofield Energy Treatment) under similar laboratory conditions. Later on, the control and the Biofield Energy Treated samples were kept in similar sealed conditions and characterized with the help of PSA, PXRD, DSC, TGA/DTG, FTIR, and UV-Vis techniques.

Characterization

Particle Size Analysis (PSA)

The particle size analysis of the samples was done using the wet method, which is conducted on Malvern Mastersizer 3000 (UK), with a detection range between 0.01 µm to 3000 µm [31]. In this method, the sample unit (Hydro MV) was filled with light liquid paraffin oil (act as a dispersant medium) and stirred at 2500 rpm. The refractive index values for dispersant medium and samples were 0.0 and 1.47, respectively. The measurement was taken twice after reaching obscuration between 10% and 20%, followed by averaging the two measurements. The analysis shows d (0.1) µm, d(0.5) µm, d(0.9) µm values that represent the particle diameter corresponding to 10%, 50%, and 90% of the cumulative distribution. The calculations were done by using software Mastersizer V3.50.

The percent change in particle size (d) for d_{10}, d_{50}, and d_{90} was calculated using the following equation 1:

$$\%\ \text{change in particle size} = \frac{[d_{Treated} - d_{Control}]}{d_{Control}} \times 100 \quad ..(1)$$

Where, $d_{Control}$ and $d_{Treated}$ are the particle size (µm) for at below 10% level (d_{10}), 50% level (d_{50}), and 90% level (d_{90}) of the control and the Biofield Energy Treated samples, respectively.

Percent change in surface area (S) was calculated using the following equation 2:

$$\%\ \text{change in surface area} = \frac{[S_{Treated} - S_{Control}]}{S_{Control}} \times 100 \quad ...(2)$$

Where, $S_{Control}$ and $S_{Treated}$ are the surface area of the control and the Biofield Energy treated cholecalciferol, respectively.

Powder X-ray Diffraction (PXRD) Analysis

The PXRD analysis of samples of cholecalciferol was done using PANalytical X'Pert3 powder X-ray diffractometer, UK. The copper line was used as the source of radiation for diffraction of the analyte at 0.154 nm X-ray wavelength that is running at 40 mA current

and 45 kV voltage. The instrument uses a scanning rate of 18.87°/second over a 2q range of 3-90° and the ratio of Kα-2 and Kα-1 was 0.5 (k, equipment constant). The data was collected using X'Pert data collector and X'Pert high score plus processing software in the form of a chart of the Bragg angle (2θ) *vs.* intensity (counts per second), and a detailed table containing information on peak intensity counts, d value (Å), full width half maximum (FWHM) (°2θ), relative intensity (%), and area (cts*°2θ). The crystallite size (G) was calculated by using the Scherrer equation (3) as follows:

$$G = k\lambda/(b\text{Cos}\theta) \quad ...(3)$$

Where, k is the equipment constant (0.5), λ is the X-ray wavelength (0.154 nm); b in radians is the full -width at half of the peaks, and θ is the corresponding Bragg angle.

Percent change in crystallite size (G) of cholecalciferol was calculated using the following equation 4:

$$\%\ \text{change in crystallite size} = \frac{[G_{\text{Treated}} - G_{\text{Control}}]}{G_{\text{Control}}} \times 100 \quad ...(4)$$

Where, $G_{Control}$ and $G_{Treated}$ are the crystallite size of the control and the Biofield Energy Treated cholecalciferol samples, respectively.

Differential Scanning Calorimetry (DSC)

The DSC analysis of the samples was performed using DSC Q2000 differential scanning calorimeter, USA, under the dynamic nitrogen atmosphere with a flow rate of 50 mL/min. For analysis, 2-4 mg sample was weighed and sealed in Aluminum pans. Further, it was equilibrated at 30°C and heated up to 450°C at the heating rate of 10° C/min under Nitrogen gas as a purge atmosphere [33]. The value for onset, end set, peak temperature, peak height (mJ or mW), peak area, and change in heat (J/g) for each peak was recorded. Later on, the percent change in melting temperature (T) of the control and the Biofield Energy Treated samples were calculated using the following equation 5:

$$\%\ \text{change in melting temperature} = \frac{[T_{\text{Treated}} - T_{\text{Control}}]}{T_{\text{Control}}} \times 100 \quad ...(5)$$

Where, $T_{Control}$ and $T_{Treated}$ are the melting temperatures of the control and the Biofield Energy Treated cholecalciferol samples, respectively.

Also, the percent change in the latent heat of fusion (ΔH) was calculated using the following equation 6:

$$\%\ \text{change in latent heat of fusion} = \frac{[\Delta H_{\text{Treated}} - \Delta H_{\text{Control}}]}{\Delta H_{\text{Control}}} \times 100 \quad ...(6)$$

Where, $\Delta H_{Control}$ and $\Delta H_{Treated}$ are the latent heat of fusion of the control and treated cholecalciferol, respectively.

Thermal Gravimetric Analysis (TGA) / Differential Thermogravimetric Analysis (DTG)

TGA/DTG thermograms of control and the Biofield Energy Treated cholecalciferol samples were obtained using TGA Q500 themoanalyzer apparatus, USA under dynamic nitrogen atmosphere (50 mL/min). It involves the heating rate of 10 ºC/min from 25 °C to 800 °C and uses platinum crucible [33]. In TGA analysis, the weight loss in gram as well as percent loss for each step was recorded with respect to the initial weight of the sample. Later on, in DTG analysis, the onset, endset, peak temperature, and integral area for each peak was recorded. The percent change in weight loss (W) was calculated using the following equation 7:

$$\%\ \text{change in weight loss} = \frac{[W_{\text{Treated}} - W_{\text{Control}}]}{W_{\text{Control}}} \times 100 \quad ...(7)$$

Where, $W_{Control}$ and $W_{Treated}$ are the weight loss of the control and the Biofield Energy Treated samples, respectively.

Also, the percent change in maximum thermal degradation temperature (T_{max}) (M) was calculated using the following equation 8:

$$\%\ \text{change in } T_{max}\ (M) = \frac{[M_{\text{Treated}} - M_{\text{Control}}]}{M_{\text{Control}}} \times 100 \quad ...(8)$$

Where, $M_{Control}$ and $M_{Treated}$ are the T_{max} values of the control and the Biofield Energy Treated samples, respectively.

Fourier Transform Infrared (FT-IR) Spectroscopy

FT-IR spectroscopy of cholecalciferol was performed on Spectrum ES Fourier transform infrared spectrometer (Perkin Elmer, USA) by using pressed KBr

disk technique with the frequency array of 400-4000 cm^{-1}. The technique uses ~2 mg of the control sample and about 300 mg of KBr as the diluent to form the pressed disk followed by running the sample in the spectrometer. The same procedure was used for the Biofield Energy Treated sample [34, 35].

Ultraviolet-visible Spectroscopy (UV-Vis) Analysis

The UV-Vis spectral analysis of the control and the Biofield Energy Treated cholecalciferol samples was carried out using Shimadzu UV-2400PC SERIES with UV Probe (Shimadzu, JAPAN). The spectrum was recorded in the wavelength range of 190-800 nm using 1 cm quartz cell having a slit width of 0.5 nm. The absorbance spectra (in the range of 0.2 to 0.9) and wavelength of maximum absorbance (λ_{max}) were recorded [36, 37].

Results and Discussion

Particle Size Distribution (PSD) Analysis

PSA analysis was used to determine the particle sizes {d_{10}, d_{50}, d_{90}, and D(4, 3)} and the surface area of the control and the Biofield Energy Treated cholecalciferol samples, and the results are mentioned in Table 1. The particle size distribution of the control sample was observed at d_{10} = 103.37µm, d_{50} = 328.16µm, d_{90} = 685.18µm, and D(4, 3) = 365.12µm. On the other hand, the particle size distribution of the Biofield Energy Treated sample was observed at d_{10} = 97.37µm, d_{50} = 274.06µm, d_{90} = 565.12µm, and D(4, 3) = 305.85µm. The analysis (Table 1) showed that the particle size values at d_{10}, d_{50}, and d_{90}, and D(4, 3) in the Biofield Energy Treated sample were significantly decreased by 5.80%, 16.49%, 17.52%, and 16.23%, respectively compared to the control sample. Besides, the specific surface area (SSA) of the Biofield Energy Treated sample (35.18 m^2/Kg) was found to be significantly increased by 7.26% as compared to the control sample (32.80 m^2/Kg).

The possible reason behind such alterations in the particle sizes might be that the Trivedi Effect® might act as an external force that helps in reducing the particle size of vitamin D_3 as done in case of treatment under ball mill. Moreover, according to scientific literature, the reduced particle size and thereby, increased the surface area of any pharmaceutical solid compound further helps in improving the dissolution rate, absorption, and bioavailability profile of drugs [38, 39]. Thus, it is presumed that the Trivedi Effect® - Consciousness Energy Treated cholecalciferol might produce better bioavailability as compared to the untreated sample.

Powder X-ray Diffraction (PXRD) Analysis

The XRD diffractograms of both the samples, *i.e.,* control and the Biofield Energy Treated samples showed sharp and intense peaks. Since there were no broadening of peaks observed in diffractograms, thus it suggested the crystalline nature of both the samples. Also, the Bragg angle and other PXRD data from the diffractogram of the control sample were observed to be similar to the reported literature [40]. The PXRD data that was collected from the diffractograms, such as Bragg angle (2θ) and relative peak intensity (%) were analyzed for the determination of crystallite size (G) of both the samples. Moreover, the Scherer equation [40] was used for calculating the crystallite sizes of both the samples.

The PXRD diffractogram of the control sample showed highest peak intensity (100%) at Bragg's angle (2θ) equal to 5.0° (Table 2, entry 1); whereas, it was observed at 18.1° (Table 2, entry 11) in the diffractogram of the Biofield Energy Treated sample. Apart from that, the relative intensities of the PXRD peaks at 2θ equal to 13.7°, 18.1° and 27.0° (Table 2, entry 7, 11 and 14) in the Biofield Energy Treated sample were significantly increased by 7.38, 20.19, and 22.42%, respectively compared to the control sample. However, the relative intensities of the other PXRD peaks (Table 2, entry 1-6, 8-10, 12, and 13) in the Biofield Energy Treated sample were significantly decreased in that range from 3.16% to 42.56%, compared to the control sample.

Besides, the crystallite sizes of the Biofield Energy Treated sample at 2θ equal to 8.7°, 13.0°, 16.7°, 21.8°, and 23.7° (Table 2, entry 4, 6, 10, 12, and 13) were observed to be significantly increased in the range from 16.68% to 72.71%, with respect to the control sample. Although, the crystallite sizes of the control and the Biofield Energy Treated samples at 2θ equal to 13.7° and 14.9° (Table 2, entry 7 and 8) remained unaltered; however, the crystallite sizes of the Biofield Energy Treated sample at position 2θ equal to

Table 1. Particle size distribution of the control and the Biofield Energy Treated cholecalciferol

Test Item	d_{10} (µm)	d_{50} (µm)	d_{90} (µm)	D(4,3) (µm)	SSA(m^2/Kg)
Control	103.37	328.16	685.18	365.12	32.80
Biofield Energy Treated	97.37	274.06	565.12	305.85	35.18
Percent change* (%)	-5.80	-16.49	-17.52	-16.23	7.26

d_{10}, d_{50}, and d_{90}: particle diameter corresponding to 10%, 50%, and 90% of the cumulative distribution, D(4,3): the average mass-volume diameter, and SSA: the specific surface area; *denotes the percentage change in the Particle size distribution of the Biofield Energy Treated sample with respect to the control sample.

Table 2. PXRD data for the control and the Biofield Energy Treated cholecalciferol.

Entry No.	Bragg angle (°2q)	Relative Intensity (%)			Crystallite size (G, nm)		
		Control	Treated	% Change [a]	Control	Treated	% Change [b]
1	5.0	100.0	57.7	-42.30	49.22	43.06	-12.51
2	5.1	48.68	27.96	-42.56	49.23	43.07	-12.51
3	6.7	16.52	10.44	-36.80	34.47	26.51	-23.09
4	8.7	10.04	9.15	-8.86	31.37	43.15	37.54
5	9.0	9.89	8.47	-14.36	43.16	28.76	-33.36
6	13.0	8.93	7.88	-11.76	18.23	31.49	72.71
7	13.7	20.47	21.98	7.38	43.33	43.33	0.00
8	14.9	10.44	10.11	-3.16	34.71	34.71	0.00
9	15.5	40.74	38.53	-5.42	43.42	38.59	-11.12
10	16.7	12.0	7.28	-39.33	20.45	34.78	70.05
11	18.1	83.2	100.0	20.19	49.80	29.04	-41.69
12	21.8	30.3	25.28	-16.57	25.03	29.20	16.68
13	23.7	11.71	7.15	-38.94	21.97	35.17	60.05
14	27.0	5.04	6.17	22.42	35.40	25.28	-28.59

*denotes the percentage change in the crystallite size of the Biofield Energy Treated sample with respect to the control sample.

5.0°, 5.1°, 6.7°, 9.0°, 15.5°, 18.1°, and 27.0° (Table 2, entry 1-3, 5, 7, 9, 11, and 14) were observed to be significantly decreased in the range of 11.12% to 41.69%, compared with the control sample. Also, the average crystallite size of the Biofield Energy Treated sample was observed to be 34.72 nm, in comparison to the control sample (35.70 nm), thus showed 2.80% reduction in the crystallite size. Such changes in the relative intensities, as well as the crystallite size, indicated some alterations in the crystal morphology of the Biofield Energy Treated cholecalciferol, compared to the control sample. It could be presumed that the Trivedi Effect® - Consciousness Energy Treatment might introduce a novel polymorphic form of the cholecalciferol by using the process of energy transfer. Also, the compound's polymorph may affect the physicochemical and thermodynamic properties and thereby the drug performance, such as bioavailability and therapeutic efficacy [41, 42]. Thus, the Biofield Energy Treatment might be considered as an approach for introducing the new polymorph of cholecalciferol that may help in improving its performance. Fig 1.

Differential Scanning Calorimetry (DSC) Analysis

The DSC analysis was used for the control and the Biofield Energy Treated samples to determine their melting and decomposition pattern. The data and further analysis from the DSC thermograms (Figure 2) of control and the Biofield Energy Treated samples are presented in Table 3. The scientific literature reported that the cholecalciferol exhibited sharp endothermic peak near 86.0°C as a result of the melting; whereas, the exothermic peak near 220°C might appear due to the decomposition of cholecalciferol [43]. The DSC thermograms of both, the control and the Biofield Energy Treated cholecalciferol samples (Figure 2) showed two endothermic and one exothermic peak. It was observed from the thermograms that the Biofield Energy Treated sample showed a slight increase in the melting point (86.06°C) by 0.24% as compared to the control sample (85.85°C). However, the latent heat of fusion (ΔH) of the Biofield Energy Treated sample was observed to be significantly increased by 3.68% compared with the control sample. Hence, it might be assumed that the Biofield Energy Treated sample needs more energy to undergo the melting process. Later on, the decomposition temperature (2nd peak) in the thermogram of the Biofield Energy Treated cholecalciferol was found to be reduced by 0.29%, but the enthalpy of decomposition showed 5.79% increase as compared with the control sample.

Moreover, the 2nd broad endothermic peak (3rd peak), which was observed at 308.34°C in the control sample and 309.0°C in the Biofield Energy Treated sample, might appear as a result of the slow degradation of non-volatile intermediates developing in the process of thermal reaction. The temperature and ΔH corresponding to this peak of the Biofield Energy Treated sample was found to be increased by 0.21% and 3.62%, respectively (Table 3) compared to the control sample. The overall results suggested that the thermodynamic stability of the Biofield Energy Treated cholecalciferol was significantly increased as compared to the untreated sample.

Thermal Gravimetric Analysis (TGA) / Differential Thermogravimetric Analysis (DTG)

The TGA/DTG analysis is used here to analyze the thermal stability of the control and the Biofield Energy Treated samples with the help of their thermograms (Figures 3 and 4). Also, the TGA and DTG data and their further analysis regarding the control and the Biofield Energy Treated samples are presented in Table 4. The scientific literature reported that the TGA thermogram of cholecalciferol showed a significant weight loss at 128°C that may occur due to the boiling and possible splattering of the sample [43]. In this study, the TGA thermograms of the control and the Biofield Energy Treated samples showed three steps of thermal degradation (Figure 3). The analysis showed that the percentage weight loss in the Biofield Energy Treated cholecalciferol sample was significantly decreased by 18.58% and 89.81% in the 1st and 3rd step of degradation, respectively; however, there was a slight increase in weight loss in the 2nd step by 0.57%, compared with the control sample (Table 4).

Besides, the DTG thermograms of the control and the Biofield Energy Treated samples (Figure 4) showed a single peak. The control sample showed maximum thermal degradation temperature (T_{max}) as 299.06°C, while the Biofield Energy Treated sample showed more stability, and T_{max} was observed at 304.53°C. Thus, the analysis reported that the T_{max} of

Table 3. Comparison of DSC data between the control and the Biofield Energy Treated cholecalciferol.

Sample	Melting point/Decomposition Temperature (°C)			ΔH (J/g)		
	1st Peak	2nd Peak	3rd Peak	1st Peak	2nd Peak	3rd Peak
Control	85.85	220.58	308.34	60.40	134.7	53.91
Biofield Energy Treated	86.06	219.95	309.00	62.62	142.5	55.86
% Change*	0.24	-0.29	0.21	3.68	5.79	3.62

ΔH: Latent heat of fusion/Enthalpy of decomposition, *denotes the percentage change of the Biofield Energy Treated sample with respect to the control sample.

Table 4. Thermal degradation steps of the control and the Biofield Energy Treated cholecalciferol.

Sample	TGA Weight loss (%)				DTG
	1st step	2nd step	3rd step	Total	T_{max} (°C)
Control	1.846	98.00	0.363	100.0	299.06
Biofield Energy Treated	1.503	98.56	0.037	100.0	304.53
% change*	-18.58	0.57	-89.81	0.00	1.83

T_{max}: Maximum thermal degradation temperature, *denotes the percentage change in the weight loss of the Biofield Energy Treated sample with respect to the control sample.

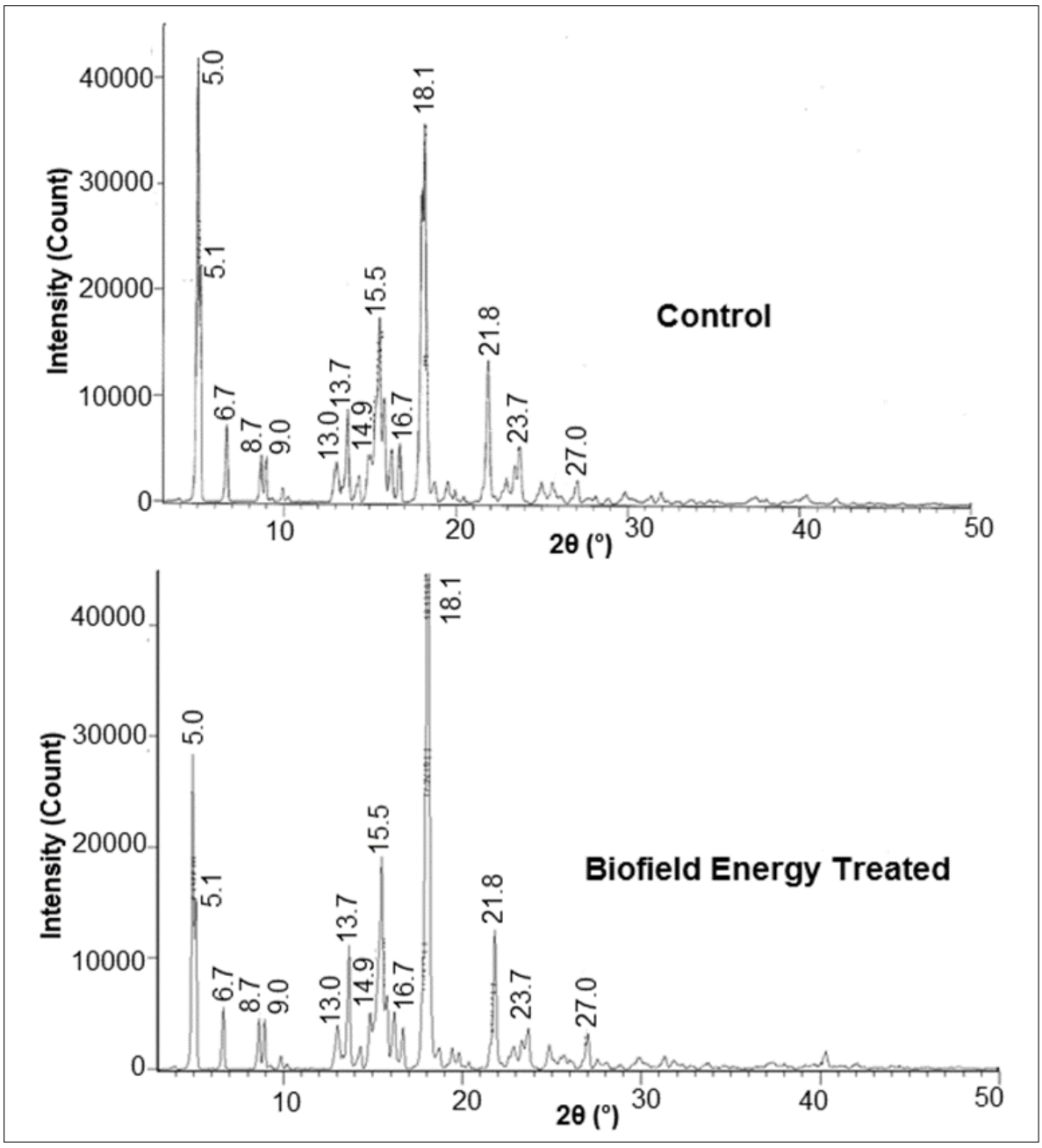

Figure 1. XRD diffractograms of the control and the Biofield Energy Treated cholecalciferol.

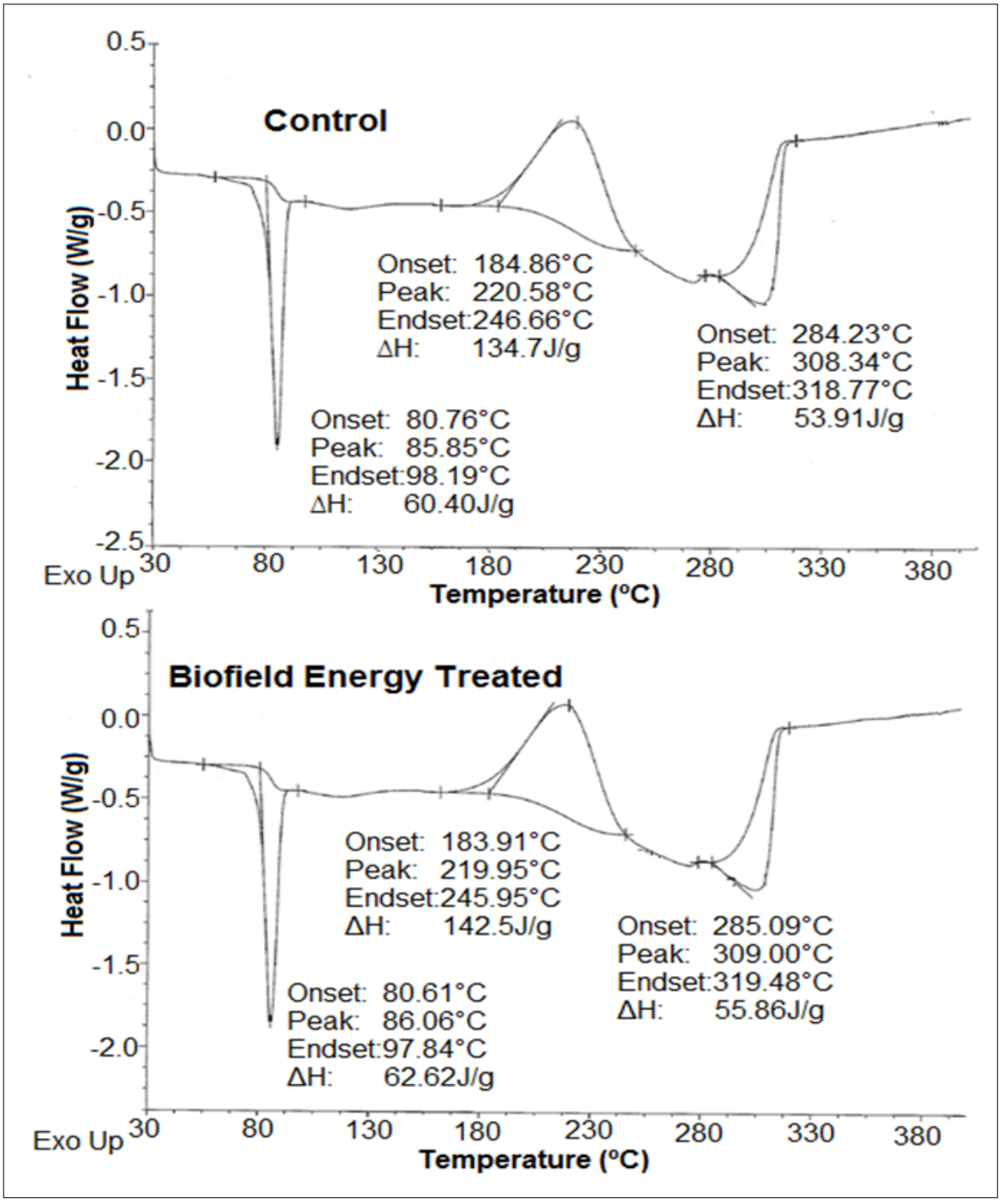

Figure 2. DSC thermograms of the control and the Biofield Energy Treated cholecalciferol.

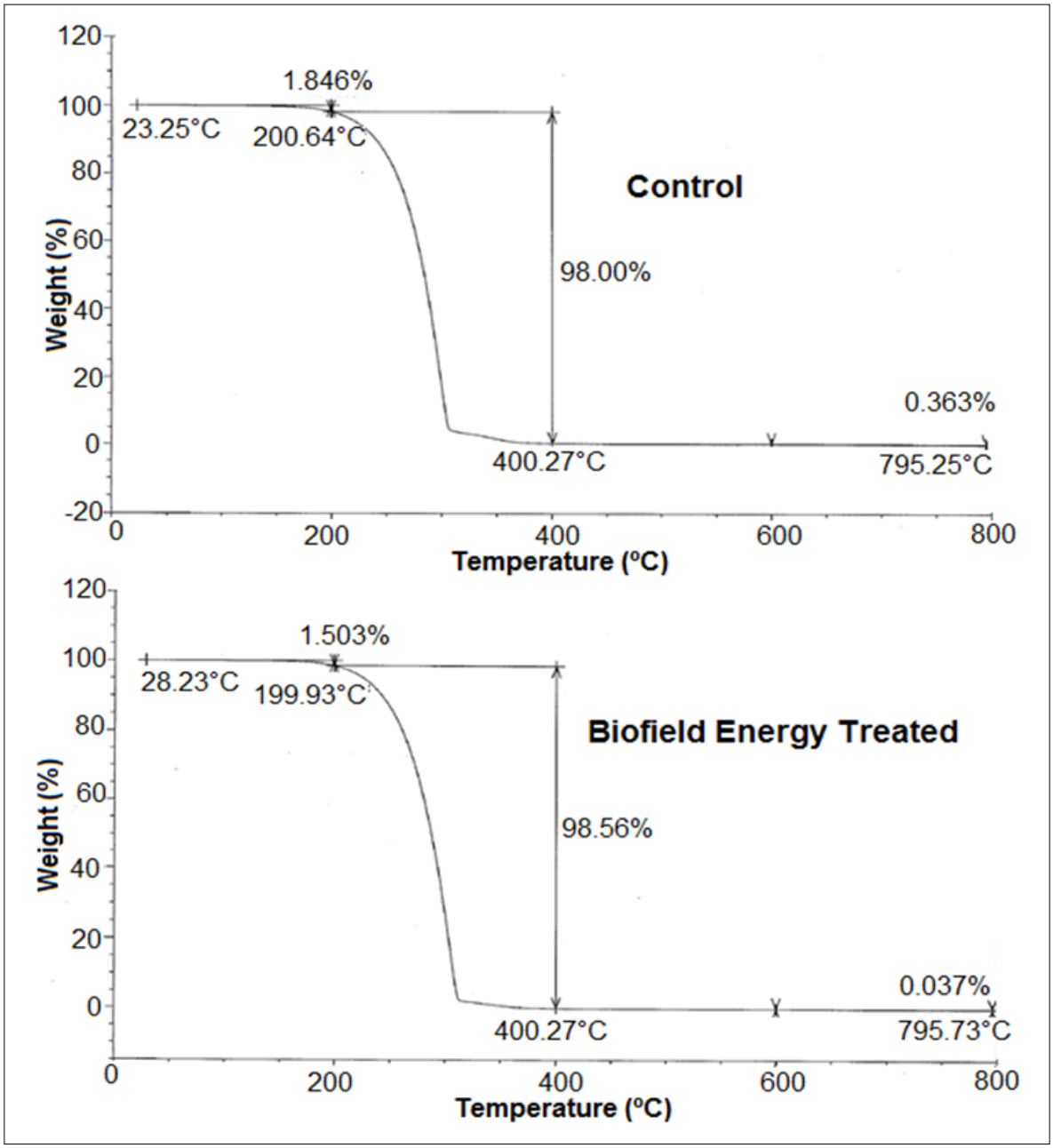

Figure 3. TGA thermograms of the control and the Biofield Energy Treated cholecalciferol

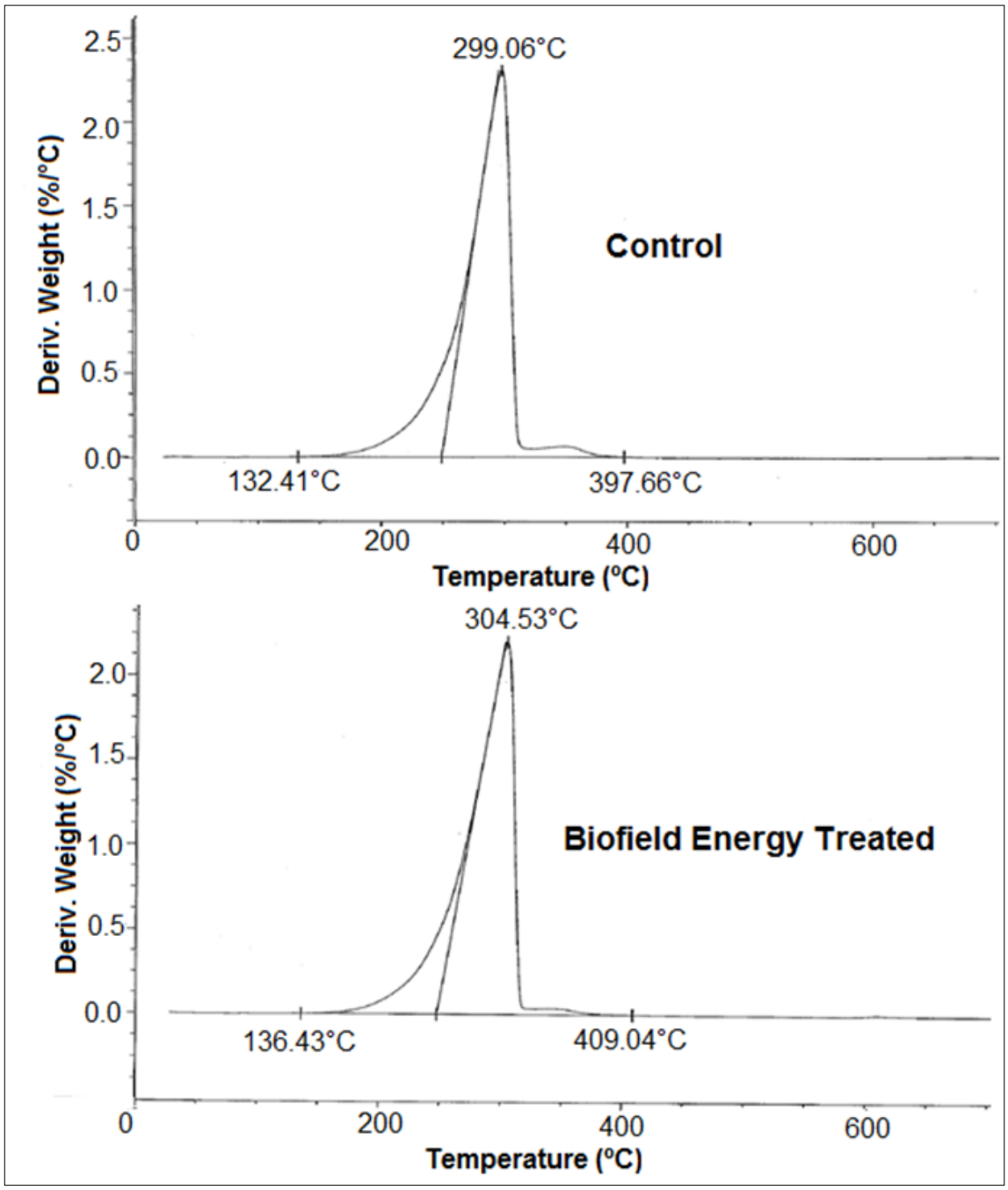

Figure 4. DTG thermograms of the control and the Biofield Energy Treated cholecalciferol.

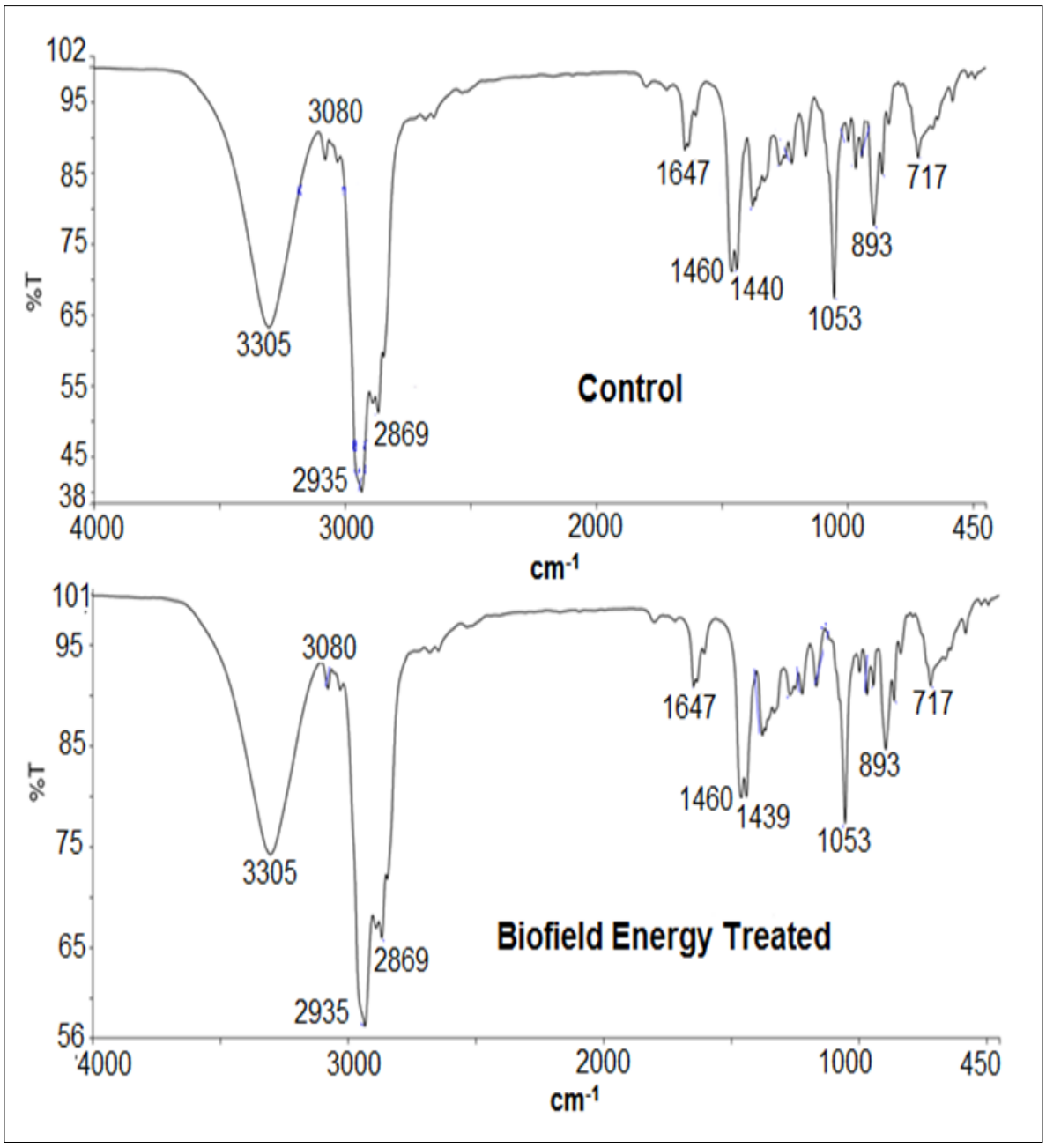

Figure 5. FT-IR spectra of the control and the Biofield Energy Treated cholecalciferol.

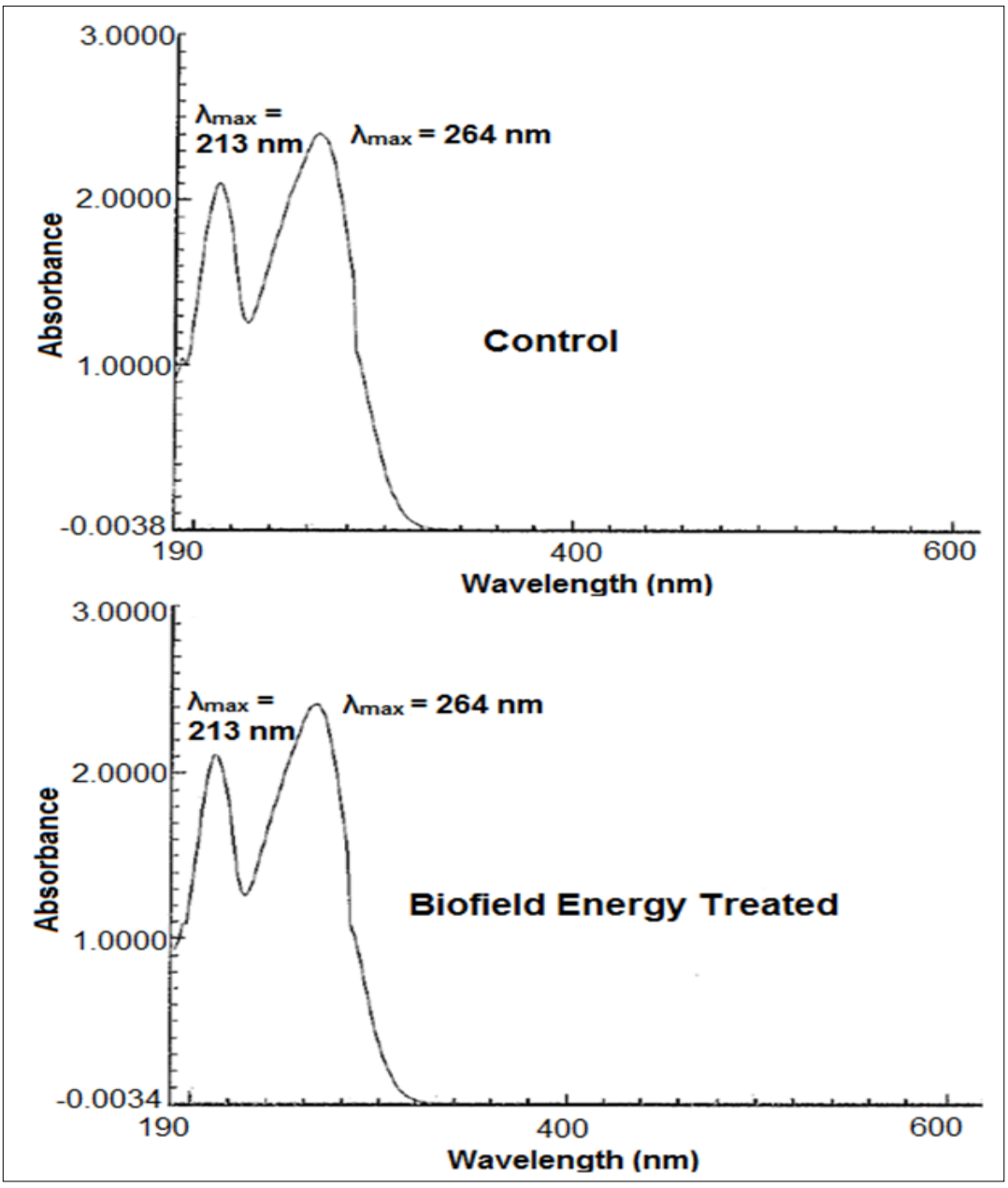

Figure 6. UV-vis spectra of the control and the Biofield Energy Treated cholecalciferol.

the Biofield Energy Treated cholecalciferol was significantly increased by 1.83% as compared to the control sample. Overall, the TGA/DTG analysis represented that the thermal stability of the Biofield Energy Treated cholecalciferol was significantly increased as compared to the control sample.

Fourier Transform Infrared (FT-IR) Spectroscopy

The FT-IR spectra of both the control as well as the Biofield Energy Treated cholecalciferol samples are presented in Figure 5. The FT-IR spectra of both the samples showed a clear stretching and bending peak in the functional group as well as the fingerprint region.

The spectra of both the samples showed broad peaks near 3305 cm^{-1} in the functional group area and were assigned to O-H stretching. Furthermore, the aromatic C-H stretching was observed at 3080 cm^{-1} in case of both, the control and the Biofield Energy Treated samples. The peaks due to aliphatic C-H stretching were observed at 2935 cm^{-1} and 2869 cm^{-1} in the spectra of both, the control and the Biofield Energy Treated sample. Besides, there was the presence of variable peak at 1647cm^{-1} in the spectra of control and the Biofield Energy Treated cholecalciferol that was due to C=C stretching. Moreover, the spectra of control sample showed aromatic C=C stretching frequency at 1440 and 1460 cm^{-1}, which was observed to be similar in the Biofield Energy Treated sample (1439 and 1460 cm^{-1}). The FTIR techniques can be used to monitor the stability, durability and to understand the chemical and surface chemistry in various types of membrane toward their performance. FTIR analysis is crucial to support the justification of the changes in their properties and performance in various applications [34, 35, 44]. The overall FT-IR analysis showed that the fingerprint region of the spectra of control and the Biofield Energy Treated sample was similar and no alteration in the vibrational frequencies was observed among both the spectra. Thus, it is presumed that the structural properties of the Biofield Energy Treated sample remained the same as that of the control sample.

Ultraviolet-visible Spectroscopy (UV-Vis) Analysis

The UV-visible spectra of both the control and the Biofield Energy Treated cholecalciferol samples are presented in Figure 6. The UV spectrum of both the samples *i.e.,* the control and the Biofield Energy Treated cholecalciferol sample showed the maximum absorbance at 213 nm (λ_{max}) and 264 nm (λ_{max}). Thus, it is assumed that the electronic transitions between the highest occupied molecular orbital and lowest unoccupied molecular orbital of the Biofield Energy Treated sample were the same as that of the untreated cholecalciferol sample. UV–visible spectrophotometry is an important for the detection of various naturally occurring groups of substances like flavonoids, phenolic acids, anthraquinones, and coumarins due to their sharp characteristic UV spectra [45, 46].

Conclusions

The study concluded that the Trivedi Effect® - Consciousness Energy Treatment has a considerable impact on the physicochemical and thermal properties of cholecalciferol such as, particle size, surface area, crystallite size, and thermodynamic stability. The particle size values at d_{10}, d_{50}, d_{90}, and D(4, 3) in the Biofield Energy Treated sample were observed to be significantly decreased by 5.80%, 16.49%, 17.52%, and 16.23%, respectively compared to the control sample. Also, the specific surface area (SSA) of the Biofield Energy Treated cholecalciferol sample was significantly increased by 7.26% as compared to the control sample. Such alterations in the particle size and surface area may help in better solubility, dissolution, and absorption of the Biofield Energy Treated cholecalciferol as compared to the untreated sample. Moreover, the relative intensities of the characteristic peaks in the Biofield Energy Treated sample showed significant alterations in the range from -42.56% to 22.42% compared with the control sample. Similarly, the crystallite sizes of the Biofield Energy Treated sample across various planes were observed to be significantly altered from -41.69% to 72.71% compared with the control sample. The average crystallite size of the Biofield Energy Treated sample was 34.72 nm, which showed 2.80% reduction when compared to the average crystallite size of the control sample (35.70 nm). Such changes in the relative intensities as well as the crystallite size of the Biofield Energy Treated sample indicated that the Trivedi Effect® - Consciousness Energy Treatment might be able to produce a polymorphic form of the cholecalciferol that may further affect its dissolution and bioavailability profile. Later on,

the DSC analysis revealed that the melting point of the treated sample was slightly increased (0.24%) with a significant increase in ΔH (3.68%) compared to the control sample. Also, the decomposition temperature and corresponding ΔH of the Biofield Energy Treated sample were altered by -0.29% and 5.79%, respectively as compared to the control sample. Moreover, the melting temperature and ΔH regarding the third peak in the Biofield Energy Treated sample were increased by 0.21% and 3.62%, respectively compared to the control sample. Besides, the TGA analysis showed that the weight loss in the 1st and 3rd steps of degradation of the Biofield Energy Treated sample were significantly decreased by 18.58% and 89.81%, respectively compared with the control sample. Consequently, the DTG analysis revealed 1.83% increase in T_{max} of the Biofield Energy Treated cholecalciferol compared to the control sample. Overall, the thermal analysis indicated that the thermodynamic stability of the Biofield Energy Treated cholecalciferol showed significant improvement as compared to the control sample. Such improved stability may help in better storage and transportation of the compound as compared to the untreated sample. Thus, it is concluded that the Consciousness Energy Treatment (the Trivedi Effect®) might be advantageous as it helps in producing a polymorphic form of cholecalciferol that possesses the improved solubility, dissolution, and absorption along with improved stability and bioavailability profile as compared to the control sample. Hence, the Biofield Energy Treated cholecalciferol might be used in designing such formulations that showed a better response in the treatment and prevention of vitamin D deficiency and other associated problems.

Acknowledgements

The authors are grateful to GVK Biosciences Pvt. Ltd., Trivedi Science, Trivedi Global, Inc., Trivedi Testimonials, and Trivedi Master Wellness for their assistance and support during this work.

References

1. Sunyecz JA (2008) The use of calcium and vitamin D in the management of osteoporosis. Ther Clin Risk Manag 4: 827-836.
2. Heaney RP (2005) The vitamin D requirement in health and disease. J Steroid Biochem Mol Biol 97: 13-19.
3. Bikle DD (2012) Vitamin D and Bone. Curr Osteoporos Rep 10: 151-159.
4. Adams JS, Modlin RL, Diz MM, Barnes PF (1989) Potentiation of the macrophage 25-hydroxyvitamin D-1-hydroxylation reaction by human tuberculous pleural effusion fluid. J Clin Endocrinol Metab 69: 457-460.
5. Holick MF (2004) Sunlight and vitamin D for bone health and prevention of autoimmune diseases, cancers, and cardiovascular disease. Am J Clin Nutr 80:1678-1688.
6. Institute of Medicine (1997) Dietary reference intakes for calcium, phosphorus, magnesium, vitamin D, and fluoride. National Academy of Sciences, Washington, DC.
7. Bikle DD (2014) Vitamin D metabolism, mechanism of action, and clinical applications. Chemistry & biology 21: 319-329.
8. Aloia JF, Patel M, Dimaano R, Li-Ng M, Talwar SA, Mikhail M, Pollack S, Yeh JK (2008) Vitamin D intake to attain a desired serum 25-hydroxyvitamin D concentration. Am J Clin Nutr 87: 1952-1958.
9. Holick MF (2007) Vitamin D deficiency. N Engl J Med 357: 266-281.
10. Bachrach S, Fisher J, Parks JS (1979) An outbreak of vitamin D deficiency rickets in a susceptible population. Pediatrics 64: 871-877.
11. Koshy KT, Beyer WF (1984) Vitamin D_3 (Cholecalciferol) in Analytical Profiles of Drug Substances, Florey K (Ed.), Vol 13, Academic Press, Inc., Orlando, USA, pp. 656-707.
12. Collins ED, Norman AW (2001) Vitamin D in Handbook of Vitamins, 3rd Edn., Rucker RB, Suttie JW, McCormick DB, Machlin LJ, Marcel Dekker, Inc., New York, pp. 51-114.
13. Chereson R (2009). Bioavailability, bioequivalence, and drug selection. In: Makoid CM, Vuchetich PJ, Banakar UV (Eds) Basic pharmacokinetics (1st Edn) Pharmaceutical Press, London.
14. Hammerschlag R, Levin M, McCraty R, Bat N, Ives JA, Lutgendorf SK, Oschman JL (2015) Biofield Physiology: A Framework for an Emerging Discipline.

Glob Adv Health Med 4: 35-41.

15. Trivedi MK, Mohan TRR (2016) Biofield energy signals, energy transmission and neutrinos. American Journal of Modern Physics 5: 172-176.
16. Warber SL, Cornelio D, Straughn, J, Kile G (2004). Biofield energy healing from the inside. J Altern Complement Med 10: 1107-1113.
17. Rubik B, Muehsam D, Hammerschlag R, Jain S (2015) Biofield science and healing: history, terminology, and concepts. Glob Adv Health Med 4: 8-14.
18. Barnes PM, Bloom B, Nahin RL (2008) Complementary and alternative medicine use among adults and children: United States, 2007. Natl Health Stat Report 12: 1-23.
19. Trivedi MK, Tallapragada RM, Branton A, Trivedi D, Nayak G, Latiyal O, Jana S (2015) The potential impact of biofield energy treatment on the atomic and physical properties of antimony tin oxide nanopowder. American Journal of Optics and Photonics 3: 123-128.
20. Trivedi MK, Tallapragada RM, Branton A, Trivedi D, Nayak G, Latiyal O, Jana S (2015) Physical, atomic and thermal Properties of Biofield Treated Lithium Powder. J Adv Chem Eng 5: 136.
21. Trivedi MK, Tallapragada RM, Branton A, Trivedi D, Nayak G, Latiyal O, Jana S (2015) Characterization of physical and structural properties of aluminium carbide powder: Impact of biofield treatment. J Aeronaut Aerospace Eng 4: 142.
22. Trivedi MK, Branton A, Trivedi D, Shettigar H, Bairwa K, Jana S (2015) Fourier transform infrared and ultraviolet-visible spectroscopic characterization of biofield treated salicylic acid and sparfloxacin. Nat Prod Chem Res 3: 186.
23. Trivedi MK, Patil S, Shettigar H, Bairwa K, Jana S (2015) Effect of biofield treatment on spectral properties of paracetamol and piroxicam. ChemSci J 6: 98.
24. Trivedi MK, Branton A, Trivedi D, Nayak G, Balmer AJ, Anagnos D, Kinney JP, Holling JM, Balmer JA, Duprey-Reed LA, Parulkar VR, Panda P, Sethi KK, Jana S (2017) Study of the energy of consciousness healing treatment on physical, structural, thermal, and behavioral properties of zinc chloride. Modern Chemistry 5: 19-28.
25. Trivedi MK, Branton A, Trivedi D, Nayak G, Wellborn BD, Smith DL, Koster DA, Patric E, Singh J, Vagt KS, Callas KJ, Panda P, Sethi KK, Jana S (2017) Characterization of physicochemical, thermal, structural, and behavioral properties of magnesium gluconate after treatment with the Energy of Consciousness. International Journal of Pharmacy and Chemistry 3: 1-12.
26. Trivedi MK, Branton A, Trivedi D, Nayak G, Bairwa K, Jana S (2015) Physicochemical and spectroscopic characteristics of biofield treated *p*-chlorobenzophenone. American Journal of Physical Chemistry 4: 48-57.
27. Trivedi MK, Branton A, Trivedi D, Nayak G, Bairwa K, Jana S (2015) Physical, thermal and spectroscopical characterization of biofield treated triphenylmethane: An impact of biofield treatment. J Chromatogr Sep Tech 6: 292.
28. Dodon J, Trivedi MK, Branton A, Trivedi D, Nayak G, Gangwar M, Jana S (2017) The study of biofield energy treatment based herbomineral formulation in skin health and function. American Journal of BioScience. 5: 42-53.
29. Kinney JP, Trivedi MK, Branton A, Trivedi D, Nayak G, Mondal SC, Jana S (2017) Overall skin health potential of the biofield energy healing based herbomineral formulation using various skin parameters. American Journal of Life Sciences 5: 65-74.
30. Trivedi MK, Branton A, Trivedi D, Nayak G, Mondal SC, Jana S (2015) Evaluation of biochemical marker - glutathione and DNA fingerprinting of biofield energy treated *Oryza sativa*. American Journal of BioScience 3: 243-248.
31. Trivedi MK, Branton A, Trivedi D, Nayak G, Gangwar M, Jana S (2016) Molecular analysis of biofield treated eggplant and watermelon crops. Adv Crop Sci Tech 4: 208.
32. Trivedi MK, Branton A, Trivedi D, Nayak G, Mondal SC, Jana S (2015) Effect of Biofield treated energized water on the growth and health status in

chicken (*Gallus gallus domesticus*). Poult Fish WildlSci 3: 140.

33. Trivedi MK, Branton A, Trivedi D, Nayak G, Plikerd WD, Surguy PL, Kock RJ, Piedad RB, Callas RP, Ansari SA, Barrett SL, Friedman S, Christie SL, Chen Liu S-M, Starling SE, Jones S, Allen SM, Wasmus SK, Benczik TA, Slade TC, Orban T, Vannes VL, Schlosser VM, Albino YSY, Panda P, Sethi KK, Jana S (2017) A systematic study of the biofield energy healing treatment on physicochemical, thermal, structural, and behavioral properties of iron sulphate. International Journal of Bioorganic Chemistry. 2: 135-145.
34. S. Suresh, S. Karthikeyan, K. Jayamoorthy (2016) FTIR and multivariate analysis to study the effect of bulk and nano copper oxide on peanut plant leaves, Journal of Science: Advanced Materials and Devices 1(3): 343-350.
35. S. Suresh, S. Karthikeyan, K. Jayamoorthy (2016) Effect of bulk and nano-Fe2O3 particles on peanut plant leaves studied by Fourier transform infrared spectral studies, Journal of Advanced Research 7(5): 739-747.
36. S Suresh, K Jayamoorthy, S Karthikeyan (2018) Switch-on fluorescence of 5-amino-2- mercapto benzimidazole by Mn_3O_4 nanoparticles: Experimental and theoretical approach, Journal of Luminescence 198: 28-33.
37. J. Jayabharathi, V. Thanikachalam, V. Kalaiarasi, K. Jayamoorthy (2014) Enhancing photoluminescent behavior of 2-(naphthalen-1-yl)-1,4,5-triphenyl-1Himidazole by ZnO and Bi_2O_3, Spectrochim.Acta Part A 118: 182-186.
38. Zhao Z, Xie M, Li Y, Chen A, Li G, Zhang J, Hu H, Wang X, Li S (2015) Formation of curcumin nanoparticles *via* solution enhanced dispersion by supercritical CO_2. Int J Nanomedicine 10: 3171-3181.
39. Raza K, Kumar P, Ratan S, Malik R, Arora S (2014) Polymorphism: The phenomenon affecting the performance of drugs. SOJ Pharm Pharm Sci 1: 10.
40. Brittain HG (2009) Polymorphism in pharmaceutical solids in Drugs and Pharmaceutical Sciences. (2nd Edn) Informa Healthcare USA, Inc., New York.
41. Mosharrof M, Nystrom C (1995) The effect of particle size and shape on the surface specific dissolution rate of microsized practically insoluble drugs. Int J Pharm 122: 35-47.
42. Chereson R (2009) Bioavailability, bioequivalence, and drug selection. In: Makoid CM, Vuchetich PJ, Banakar UV (Eds) Basic pharmacokinetics (1st Edn) Pharmaceutical Press, London.
43. Koshy KT, Beyer WF (1984) Vitamin D_3 (Cholecalciferol) in Analytical Profiles of Drug Substances, Florey K (Ed.), Vol 13, Academic Press, Inc., Orlando, USA, pp. 656-707.
44. Berthomieu, C., Hienerwadel, R (2009) Fourier transform infrared (FTIR) spectroscopy. Photosynth Res 101: 157–170.
45. C. Karunakaran, J. Jayabharathi, R. Sathishkumar, K. Jayamoorthy (2013) Interaction of fluorescent sensor with superparamagnetic iron oxide nanoparticles. Spectrochim.Acta Part A: 110: 151-156.
46. F. Sánchez Rojas J.M. Cano Pavón, in Encyclopedia of Analytical Science (Second Edition), 2005 Spectrophotometry, biochemical applications.